Importance of Interorbital Charge Transfers for the Metal-to-Insulator Transition of $BaVS_3$

Frank Lechermann,[1,2] Silke Biermann,[1] and Antoine Georges[1]
[1]*CPHT École Polytechnique, 91128 Palaiseau Cedex, France*
[2]*LPT-ENS, 24 Rue Lhomond, 75231 Paris Cedex 05, France*
(Received 17 September 2004; published 29 April 2005)

The underlying mechanism of the metal-to-insulator transition (MIT) in $BaVS_3$ is investigated, using dynamical mean-field theory in combination with density functional theory. It is shown that correlation effects are responsible for a strong charge redistribution, which lowers the occupancy of the broader A_{1g} band in favor of the narrower E_g bands and thereby substantially modifies the Fermi surface. This resolves several discrepancies between band theory and the experimental findings, such as the observed value of the charge-density-wave ordering vector associated with the MIT, and the presence of local moments in the metallic phase.

DOI: 10.1103/PhysRevLett.94.166402 PACS numbers: 71.30.+h, 71.10.Fd, 71.15.Mb, 75.30.Cr

The structural, electronic, and magnetic properties of the vanadium sulfide compound $BaVS_3$ raise several puzzling questions [1,2]. At room temperature, this material crystallizes in a hexagonal ($P6_3/mmc$) structure [3], in which straight chains of face-sharing VS_6 octahedra are directed along the c axis. At $T_S \sim 240$ K the crystal structure transforms into an orthorhombic ($Cmc2_1$) structure [4], thereby creating an anisotropy in the ab plane and a zigzag distortion of the VS_3 chains in the bc plane. Additionally, the Hall coefficient changes sign from negative to positve at T_S [2]. On further cooling, the system displays a metal-to-insulator transition (MIT) at $T_{MIT} \sim 70$ K. Remarkably, this transition is second order and is not accompanied by magnetic ordering. Only below $T_X \sim 30$ K indications for an incommensurate antiferromagnetic order exist [5].

Forró *et al.* [6] have found that the MIT can be driven to $T = 0$ by applying pressure [7]. Further recent experiments [8,9] have demonstrated that the MIT is in fact associated with a structural transition. These studies establish that a commensurate structural modulation sets in, corresponding to a reduced wave vector $\mathbf{q} = (1, 0, \frac{1}{2})_O$ in the orthorhombic cell. Furthermore, x-ray diffuse scattering experiments [9] reveal a large fluctuation regime with critical wave vector $\mathbf{q}_c = 0.5\mathbf{c}^*$ (here $\mathbf{c}^*$ is the reciprocal unit vector along the orthorhombic c axis), extending up to 170 K into the metallic phase. In the same temperature range the Hall coefficient is strongly increasing [2]. This regime might be interpreted as a precursor of the charge-density-wave (CDW) instability, reminiscent of the large fluctuations in a quasi-one-dimensional (1D) metal in the vicinity of a Peierls transition. It should be kept in mind, however, that the conduction anisotropy within the system is not strongly pronounced ($\sigma_c/\sigma_a \sim 3$–4) [10], making 1D interpretations questionable. The ''metallic'' phase above T_{MIT}displays several other unusual properties [7,10]. The resistivity is rather high (a few mΩ cm) and metalliclike ($d\rho/dT > 0$) only above a weak minimum at $\sim$150 K, below which it increases upon further cooling. Most interestingly, this phase displays local moments, as revealed by the Curie-Weiss form of the magnetic susceptibility. The effective moment corresponds approximately to one localized spin-1/2 per 2 V sites. Since the formal valence is V^{4+}, corresponding to one electron in the $3d$ shell, this can be interpreted as the effective localization of half of the electrons. At T_{MIT}, the susceptibility rapidly drops, and the electronic entropy is strongly suppressed [11].

In the hexagonal phase the low-lying V($3d$) levels consist of an A_{1g} state and two degenerate E_g states. A further splitting of the degenerate states occurs in the orthorhombic phase. First-principles calculations of the electronic structure, based on density functional theory (DFT) in the local (spin) density approximation [L(S)DA], have been performed in Refs. [12–14]. For both phases the calculations yield a V($3d$)-S($3p$) hybridization which is strong enough to account for the weak anisotropy of the transport properties. No band-gap opening has been reached within L(S)DA. Instead, very narrow E_g bands right at the Fermi level, and a nearly filled dispersive band with mainly A_{1g} character extending along c^*, have been found, consistent with a simple model proposed early on by Massenet *et al.* [15]. However, the LDA filling of the E_g bands is too low to account for the observed local moment in the metallic phase. The nature of the CDW instability is also left unexplained. Indeed, the norm of the Fermi wave vector of the broad A_{1g} band is found to be $2k_F^{LDA} \simeq 0.94c^*$ [13], while the observed wave vector of the instability is $\mathbf{q}_c = 0.5\mathbf{c}^*$ [9]. Therefore, the picture of a CDW at $q_c = 2k_F$ associated only with the A_{1g} band is untenable within LDA. A recent x-ray study [16] in fact suggests that below the MIT a superposition of a dominant $2k_F$ and a smaller $4k_F$ displacement wave exists. Thus it is likely that the E_g states also participate in the instability. Still the LDA band structure does not provide a Fermi-surface nesting that is in line with experimental findings. Hence, *ab initio* L(S)DA calculations are not sufficient to explain the complex electronic structure of $BaVS_3$. By using static DFT + U schemes a band gap was obtained [17]. However, this required to enforce magnetic order, hence leaving unanswered the question of the mechanism of

the transition into the paramagnetic insulator. (Without magnetic order, the filling of the A_{1g} band is further *increased* within static DFT + U [17].)

In this Letter, we present calculations in the framework of dynamical mean-field theory (DMFT), using the LDA electronic structure as a starting point. On the basis of this LDA + DMFT treatment we propose correlation effects in a multiorbital context as an explanation for the discrepancies between band theory predictions and experiments. We show that interorbital charge transfers occur which lower the occupancy of the A_{1g} orbital in favor of the E_g's. This leads to a modified Fermi surface with a reduced $k_F(A_{1g})$. Local-susceptibility computations reveal that local moments are formed in the metallic phase due to the low quasiparticle coherence scale induced by the strong correlations (particularly for the narrower E_g bands).

Figure 1 displays the LDA band structure of $Cmc2_1$-$BaVS_3$ for the crystal data [4] at $T = 100$ K. The calculations were performed by using norm-conserving pseudopotentials and a mixed basis consisting of plane waves and localized functions [18], and results are consistent with previous work [12–14]. A symmetry-adapted V($3d$) basis $\{\phi_m\}$ was obtained by diagonalizing the orbital density matrix $n_{MM'} \sim \sum_{\mathbf{k}b} f^b_{\mathbf{k}} \langle \psi^b_{\mathbf{k}} | M \rangle \langle M' | \psi^b_{\mathbf{k}} \rangle$, where $\psi^b_{\mathbf{k}}$ stands for the pseudocrystal wave function for wave vector $\mathbf{k}$ and band b, and M, M' denote the cubic harmonics for $\ell = 2$. Being directed along the chain direction, the A_{1g} orbital has mainly d_{z^2} character. In contrast, the E_g states, linear combinations of d_{yz}, $d_{x^2-y^2}$, and d_{z^2} (E_{g1}) as well as d_{xy} and d_{xz} (E_{g2}), only weakly hybridize with their surroundings. The orbitals of the remaining e_g manifold point mainly towards the sulfur atoms, which results in a large energy splitting, leading to a smaller (larger) contribution to the occupied (unoccupied) states well below (above) ε_F. Hence, the e_g states do not have a major influence on the essential physics around the MIT. Note that in the orthorhombic (and hexagonal) structure, the unit cell contains 2 f.u., with the 2 V sites equivalent by symmetry. The high-symmetry points Γ-C-Y in the Brillouin zone (BZ) define a triangle in the $k_z = 0$ plane, and Z-E-T is the analogous shifted triangle in the $k_z = 0.5c^*$ plane. The Γ-Z line corresponds to propagation along the c axis. We have used a "fatband" representation associated with the $\{A_{1g}, E_g\}$ orbitals in Fig. 1 in which the width is proportional to the amount of orbital character of each band at a given k point. Therefrom, the narrow bands at the Fermi level can be associated with the E_g orbitals. Along Γ-Z starting at around -1 eV, a dispersive band with strong A_{1g} weight crosses ε_F close to the BZ edge. Hence the Γ-Z portion of that band is almost filled, with $2k_F \simeq 0.94c^*$ as mentioned above. The E_{g2} electron pocket at the Γ point is absent for the hexagonal phase (see also [13]). Its existence might be related to the holelike transport below T_S as revealed from Hall measurements [2]. The partial density of states (DOS) for each orbital displayed in Fig. 2 shows a rather broad A_{1g} DOS, while the E_g orbitals yield narrow peaks right at and above E_F.

Recently, it has become possible to investigate correlation effects in a realistic setting by combining LDA with DMFT [19]. Starting from the LDA Hamiltonian $H^{\mathrm{LDA}}_{mm'}(\mathbf{k})$ expressed in a localized basis set, many-body terms are introduced, leading to a self-energy matrix $\Sigma_{mm'}$ which is taken to be local ($\mathbf{k}$ independent) but fully frequency dependent. In the present work, we use a simplified implementation of this LDA + DMFT approach, which is geared at keeping those physical ingredients which are important for the physics of $BaVS_3$ close to the MIT. We work within an effective 3-band model, whereby the LDA electronic structure enters via the DOS in the relevant energy window around the Fermi level. The effective bands are derived from the symmetry-adapted $\{A_{1g}, E_g\}$ states, thus nondiagonal self-energy terms $\Sigma_{m \neq m'}$ are negligible. From a physically adequate "empirical downfolding" procedure we constructed the effective 3-band DOS. In order to meet the $3d^1$ character, the location and width (~2.2 eV) of the energy window were chosen such that the total DOS accommodates two electrons below and ten electrons above the Fermi level (per 2 V). Since the e_g bands are hardly relevant and of minor weight close to E_F, they were hybridized with the E_g bands as suggested from the resolved partial DOS in Fig. 2. The contribution of these new E_g bands was substracted from the total DOS normalized to a single formula unit of $BaVS_3$ within the chosen energy

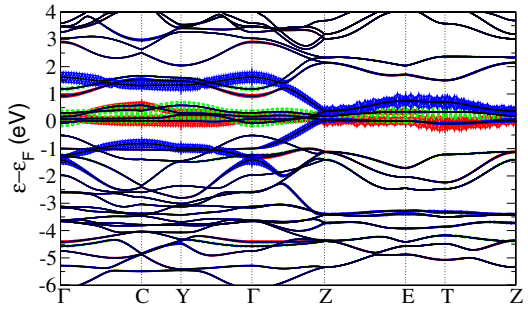

FIG. 1 (color online). LDA band structure for $Cmc2_1$-$BaVS_3$ with fatbands (see text) for the A_{1g} (blue/full solid), E_{g1} (red/full gray), and E_{g2} (green/dashed gray) orbital of the V atoms.

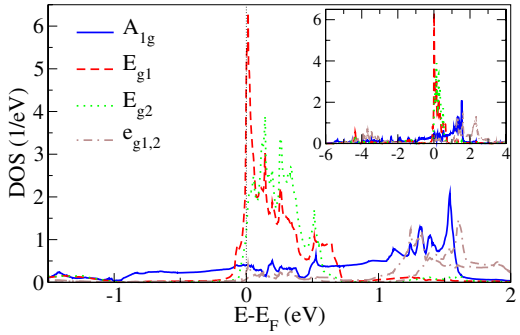

FIG. 2 (color online). Adapted basis-resolved LDA-DOS of the V($3d$) states.

window. The resulting difference was identified as the new downfolded A_{1g} band, since the A_{1g} orbital substantially hybridizes with the S($3p$) orbitals. Finally, the self-energies Σ_m associated with the effective bands are calculated from LDA + DMFT where the self-consistency condition is expressed as an integral over the effective partial DOS $D_m^{\mathrm{LDA}}(\varepsilon)$. The on-site interaction matrix was parametrized as [20] $U_{mm}^{\uparrow\downarrow} = U$, $U_{m\neq m'}^{\uparrow\downarrow} = U - 2J$, and $U_{m\neq m'}^{\uparrow\uparrow(\downarrow\downarrow)} = U - 3J$, with U the on-site Coulomb repulsion and J the local Hund's rule coupling. Note that J does not only describe the spin exchange energy, but also the reduction of U for electrons in different orbitals [20]. The DMFT local impurity problem was solved using the quantum Monte Carlo (QMC) Hirsch-Fye algorithm. Up to 128 slices in imaginary time τ and at most 10^6 sweeps were used. (The QMC calculations were performed at temperatures $T > T_{\mathrm{MIT}}$ [cf., Figs. 3–5]. As the crystal data at $T = 100$ K was used in the LDA calculations, and since the coherence scale for the broader A_{1g} band is already reached for elevated T over most of the studied range of parameters, we think that the physics close to T_{MIT} is captured.)

Figure 3(a) displays the occupancies of each orbital in the metallic regime as a function of U. In the absence of a precise determination of this parameter from either experiments (e.g., photoemission) or theory (constrained LDA methods tend to underestimate the screening for metals), we varied U over a rather large range of values. To study the interplay between U and J, we chose to fix the ratio U/J, and two series were studied: $U/J = 7$ and $U/J = 4$. The orbital occupancies in our effective 3-band model, at the LDA level (i.e., for $U = 0$) read $n(A_{1g}) = 0.712$, $n(E_{g1}) = 0.207$, and $n(E_{g2}) = 0.081$. The main effect apparent in Fig. 3(a) is that moderate correlations tend to bring the occupancies of each orbital closer to one another, i.e., to decrease the population of the "extended" orbital A_{1g} and to increase the occupancy of the E_g orbitals. For strong correlations, values close to $n(A_{1g}) \simeq n(E_{g1}) + n(E_{g2}) \simeq 0.5$ are obtained, corresponding to a half-filled band. In the absence of correlations, it pays to occupy dominantly the A_{1g} band, which provides the largest kinetic energy gain, while in the presence of correlations this has to be balanced versus the potential energy cost. The coupling J clearly favors such an interorbital charge redistribution, as also pointed out recently in the context of ruthenates [21]. For larger U, band narrowing can also promote interorbital transfers [22]. As for $BaVS_3$ it reduces the kinetic energy gain associated with the A_{1g} band. As expected, a Mott insulating state is obtained when U is larger than a strongly J-dependent critical value.

Our calculations reveal that the depletion of the A_{1g} band is accompanied by a reduction of the corresponding k_F along the Γ-Z direction. (Note that the Luttinger theorem [23] does not apply separately for each band but only relates the total Fermi-surface volume to the total occupancy.) While a full determination of the quasiparticle (QP) band structure in the interacting system requires a determination of the real-frequency self-energy, we can extract the low-energy expansion of this quantity from our QMC calculation in the form $\mathrm{Re}\Sigma_m(\omega + i0^+) \simeq \mathrm{Re}\Sigma_m(0) + \omega(1 - 1/Z_m) + \cdots$, with Z_m the QP residue associated with each orbital. The poles of the Green's function determine the QP dispersion relation: $\det[\omega_{\mathbf{k}} - \hat{Z}[\hat{H}_{\mathbf{k}}^{\mathrm{LDA}} + \mathrm{Re}\hat{\Sigma}(0) - \mu]] = 0$, with μ the chemical potential. Within our diagonal formulation the location of the Fermi wave vector for the A_{1g} sheet in the interacting system is determined by $\varepsilon_{A_{1g}}^{\mathrm{LDA}}(\mathbf{k}_F) = \mu - \mathrm{Re}\Sigma_{A_{1g}}(0)$. This quantity therefore yields the energy shift of the A_{1g} band at the Fermi-surface crossing, as compared to LDA. It is depicted in Fig. 3(b) as a function of U. In Fig. 4(a), we display the QP bands that cross the Fermi level along Γ-Z in a narrow energy range around ε_F. The QP bands are obtained from a perturbative expansion of the pole equation above, which yields $\omega_{b\mathbf{k}} = \sum_m C_{m\mathbf{k}}^b Z_m[\varepsilon_{b\mathbf{k}}^{\mathrm{LDA}} + \mathrm{Re}\Sigma_m(0) - \mu]$ with $C_{m\mathbf{k}}^b \equiv |\langle\psi_{\mathbf{k}}^b|\phi_m\rangle|^2$ the LDA orbital weight. It is evident that $k_F(A_{1g})$ is reduced in comparison to the LDA value, in line with the global charge transfer from A_{1g} to E_g. This opens new possibilities for the CDW instability, in particular, for the nesting wave vector.

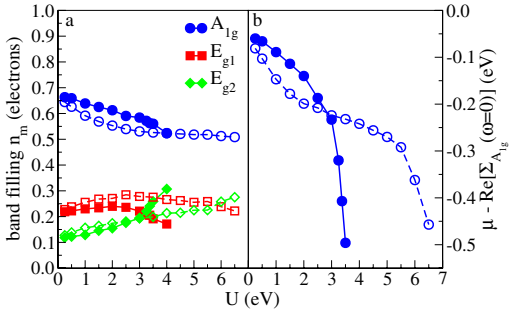

FIG. 3 (color online). (a) Band fillings at $\beta = (k_B T)^{-1} = 15\ \mathrm{eV}^{-1}$ ($T = 774$ K) for the effective bands within LDA + DMFT. (b) Corresponding shift of the Fermi level for the A_{1g} band (note that $\varepsilon_{\mathbf{k}_F}^{(\mathrm{LDA})} = 0$). Filled symbols, $U/J = 7$; open symbols, $U/J = 4$.

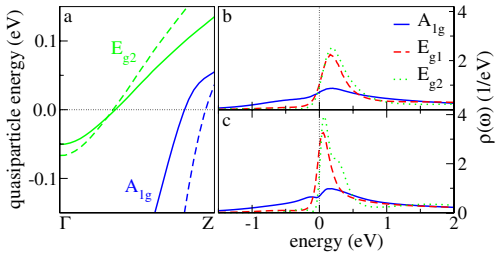

FIG. 4 (color online). LDA + DMFT spectral data for $U = 3.5$ eV, $U/J = 4$. (a) V($3d$) low-energy quasiparticle bands along Γ-Z in LDA (dashed lines) and LDA + DMFT (solid lines) for $T = 332$ K. Integrated spectral function $\rho(\omega)$ for a single formula unit of $BaVS_3$ at $T = 1160$ K (b) and $T = 332$ K (c).

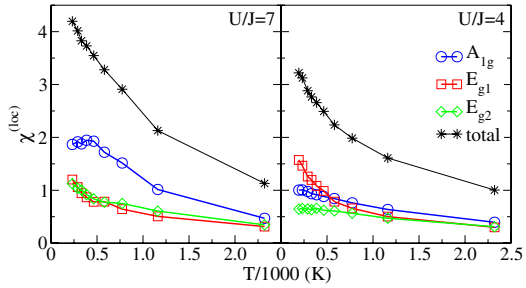

FIG. 5 (color online). T-dependent local spin susceptibilities for $U = 3.5$ eV, according to the normalization $\chi^{(\mathrm{loc})} = \int_0^\beta d\tau \times \langle \hat{S}_z(0)\hat{S}_z(\tau)\rangle$, where $\hat{S}_z$ denotes the z component of the spin operator.

The enhanced population of the E_g bands, as well as the correlation-induced reduction of its bandwidth [see Fig. 4(a)], provide an explanation for the local moments observed in the metallic phase. To support this, we have calculated (Fig. 5) the orbital-resolved local susceptibility $\chi_m^{(\mathrm{loc})} \equiv \sum_{\mathbf{q}} \mathrm{Re}[\chi_m(\mathbf{q}, \omega = 0)]$. For both values of U/J, the susceptibility of the A_{1g} band saturates to a Pauli-like value at low temperatures. In contrast, $\chi_{E_g}^{(\mathrm{loc})}$ strongly increases as T is lowered (except for the low-filled E_{g2} orbital at $U/J = 4$), since the coherence temperature below which QPs form is much lower for the E_g orbitals. Accordingly, the calculated integrated spectral functions [Fig. 4(b) and 4(c)] reveal a strong T dependence of the E_g QP peak. Some differences between the two series are clear from Fig. 5. For $U/J = 7$, the system is close to the Mott transition. Thus the A_{1g} electrons also act as local moments over part of the temperature range, while for $U/J = 4$ the T dependence of the total $\chi^{(\mathrm{loc})}$ is almost entirely due to the E_{g1} electrons. Which of the two situations is closest to the physics of $BaVS_3$ requires further investigation, albeit some experimental indications point to the second possibility [24].

In conclusion, we have shown that in $BaVS_3$ correlations lead to a modification of the LDA Fermi surface by lowering the filling of the broader A_{1g} band in favor of the narrower E_g bands. This explains the presence of local moments in the metallic phase and paves the road towards a full understanding of the CDW instability. Orbital-selective experimental probes are highly desirable to check our findings. Among several outstanding questions still open are the detailed nature of the insulating phase (especially regarding the partial suppression of local moments and the eventual magnetic ordering) as well as the suppression of T_{MIT} under pressure [6,7].

We are grateful to J.-P. Pouget and L. Forró for stimulating our interest in this material, and acknowledge useful discussions with S. Fagot, P. Foury-Leylekian, J.-P. Pouget, S. Ravy, as well as with P. Fazekas, P.A. Lee, and T. Giamarchi. Computations were performed at IDRIS Orsay. Financial support was provided by the "Psi-k f-electron" Network under Contract No. HPRN-CT-2002-00295.

Note added.—After the completion of this work, we became aware of a recent angle-resolved photoemission study of $BaVS_3$ by Mitrovic *et al.* [25] supporting our prediction of a reduced $k_F(A_{1g})$.

[1] M. H. Whangbo, H.-J. Koo, D. Dai, and A. Villesuzanne, J. Solid State Chem. **175**, 384 (2003).
[2] C. H. Booth, E. Figueroa, J. M. Lawrence, M. F. Hundley, and J. D. Thompson, Phys. Rev. B **60**, 14 852 (1999).
[3] R. Gardner, M. Vlasse, and A. Wold, Acta Crystallogr. Sect. B **25**, 781 (1969).
[4] M. Ghedira, M. Anne, J. Chenevas, M. Marezio, and F. Sayetat, J. Phys. C **19**, 6489 (1986).
[5] H. Nakamura *et al.*, J. Phys. Soc. Jpn. **69**, 2763 (2000).
[6] L. Forró *et al.*, Phys. Rev. Lett. **85**, 1938 (2000).
[7] T. Graf *et al.*, Phys. Rev. B **51**, 2037 (1995).
[8] T. Inami *et al.*, Phys. Rev. B **66**, 073108 (2002).
[9] S. Fagot, P. Foury-Leylekian, S. Ravy, J.-P. Pouget, and H. Berger, Phys. Rev. Lett. **90**, 196401 (2003).
[10] G. Mihály *et al.*, Phys. Rev. B **61**, R7831 (2000).
[11] H. Imai, H. Wada, and M. Shiga, J. Phys. Soc. Jpn. **65**, 3460 (1996).
[12] M. Nakamura *et al.*, Phys. Rev. B **49**, 16 191 (1994).
[13] L. F. Mattheiss, Solid State Commun. **93**, 791 (1995).
[14] M. H. Whangbo, H. J. Koo, D. Dai, and A. Villesuzanne, J. Solid State Chem. **165**, 345 (2002).
[15] O. Massenet *et al.*, J. Phys. Chem. Solids **40**, 573 (1979).
[16] S. Fagot *et al.*, cond-mat/0410110.
[17] X. Jiang and G. Y. Guo, Phys. Rev. B **70**, 035110 (2004).
[18] B. Meyer, C. Elsässer, F. Lechermann, and M. Fähnle, *FORTRAN 90 Program for Mixed-Basis-Pseudopotential Calculations for Crystals* (Max-Planck-Institut für Metallforschung, Stuttgart, unpublished).
[19] V. I. Anisimov, A. I. Poteryaev, M. A. Korotin, A. O. Anokhin, and G. Kotliar, J. Phys. Condens. Matter **9**, 7359 (1997); A. I. Lichtenstein and M. I. Katsnelson, Phys. Rev. B **57**, 6884 (1998).
[20] C. Castellani, C. R. Natoli, and J. Ranninger, Phys. Rev. B **18**, 4945 (1978); R. Frésard and G. Kotliar, Phys. Rev. B **56**, 12 909 (1997).
[21] S. Okamoto and A. J. Millis, Phys. Rev. B **70**, 195120 (2004).
[22] A. Liebsch and A. Lichtenstein, Phys. Rev. Lett. **84**, 1591 (2000).
[23] J. M. Luttinger, Phys. Rev. **119**, 1153 (1960).
[24] P. Fazekas *et al.*, Physica B (Amsterdam) **312**, 694 (2002).
[25] S. Mitrovic *et al.*, cond-mat/0502144.